

LINAC OPTICS CORRECTION WITH TRAJECTORY SCAN DATA*

Tong Zhang^{1,2}, Xiaobiao Huang^{2†}, Yu-Chiu Chao², Tim Maxwell²

¹University of Science and Technology of China, 96 Jinzhai Rd, Hefei, Anhui, China

²SLAC National Accelerator Laboratory, 2575 Sand Hill Road, Menlo Park, CA, USA 94025

Abstract

We proposed and tested two methods to measure and correct linac optics by scanning the beam trajectory in the horizontal and vertical phase spaces. The trajectory data are compared to tracking data in a fitting scheme, from which we can derive the quadrupole strength errors and BPM gains. A local analysis that derives the angular kicks by quadrupoles from BPM readings for places where BPMs and quadrupoles are nearby is also used.

INTRODUCTION

Global correction of linear optics in storage rings is a regular practice today. But there has not been a report of successful global optics correction for long linacs such as LCLS, SACLA, and European XFEL. These linacs consists of hundreds of quadrupole magnets along the beam path. The small errors of the quadrupoles could build up to significantly distort the optics and hence affect the machine performances. Measurement and correction of the linear optics errors in long linacs could have a big impact in improving the operation of such machines.

Global optics correction for a one-pass system has been previously demonstrated. In Ref. [1] the trajectory response matrix for a transport line is fitted to the lattice model for quadrupole errors, in a manner similar to LOCO for storage rings [2], which are then successfully used for optics correction. Ref. [3] proposed to fit turn-by-turn BPM data to the lattice model directly and tested the scheme on a section of the SPEAR3 storage ring. The turn-by-turn BPM data simply provide sampling of the phase space which can also been done in a linac. Therefore, both of the above two approaches can be used for linac optics correction.

Ref. [4] proposed a method to sample and to represent linac optics by grid scans of trajectories. Such data are suitable for lattice model fitting using the approach proposed in Ref. [3]. In this study we applied this method to LCLS trajectory scan data to derive the quadrupole errors in the model. Given the particular arrangement of BPM and quadrupole magnet positions in the LCLS, we were also able to use a local analysis to calculate quadrupole strengths. The LCLS trajectory scan data analysis in this study demonstrated that the methods can be used to calibrate linear optics for linacs.

In the following we will first describe the LCLS machine configuration and the trajectory scan data, followed by a description of the methods, and the data analysis results. A discussion and the conclusion are given toward the end.

THE LCLS TRAJECTORY SCAN DATA

LCLS consists of an injector, a 1-km linac, a transport line, and a 132-m undulator section. The trajectory scan data we obtained cover the region from linac L3 to the dump. The ideal optics of LCLS for this region is shown in Fig. 1. The beam energy ranges from 4.5 GeV to 13.6 GeV. There are 126 working BPMs and 131 quadrupole magnets in this region, respectively.

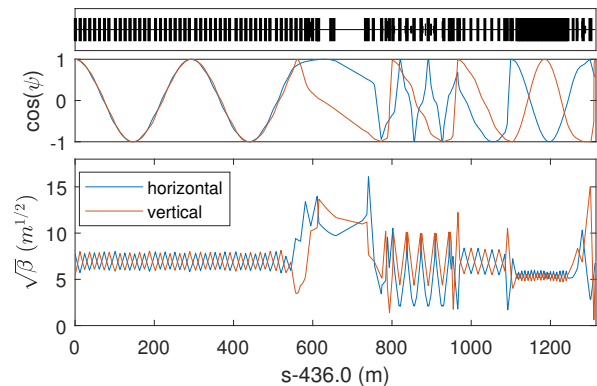


Figure 1: LCLS optics from Linac L3 to the dump.

Trajectory scan was done by using two steering magnets on each of the two transverse planes to shift the beam trajectory on a 6×6 grid in the phase space. Figure 2 shows the raw data on two nearby BPMs at the beginning of the L3 section for both the horizontal and vertical planes. Generally, the maximum trajectory deviation is $250 \mu\text{m}$ or less. At each grid point, 30 trajectories were recorded. Because the incoming beam has angle and position jittering and BPMs have random measurement errors, the 30 trajectories are dispersed around the intended grid point. The rms of the BPM readings for each grid point ranges from $5 \mu\text{m}$ to $15 \mu\text{m}$. SVD analysis of the trajectory data of the same grid point indicates that the variance is dominated by the few leading modes, whose spatial patterns show the signature of betatron phase advance. Therefore, most of the noise comes from trajectory jittering, not real BPM noise. The jittering noise does not affect the methods we used in this study.

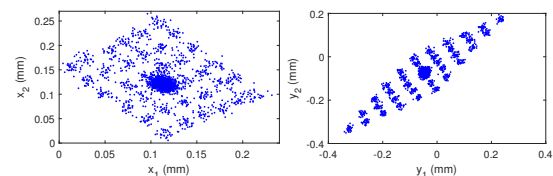


Figure 2: Trajectory scan data on BPM 10 and 12 as an example. Left: horizontal; right: vertical.

* Work supported by U.S. Department of Energy, Office of Science, Office of Basic Energy Sciences, under Contract No. DE-AC02-76SF00515

† xiahuang@slac.stanford.edu

THE DATA ANALYSIS METHODS

Two methods are used to process the trajectory scan data in order to determine the quadrupole errors in the lattice model. The first one is a local analysis that takes advantage of the special feature of the LCLS linac section that the BPMs are located inside the quadrupoles. The second method is the approach of fitting trajectory data directly to the lattice.

Local Analysis

In the LCLS linac section L3, a quadrupole and a BPM are located in the same gap between adjacent RF structures for about every 12.3 m and the BPM is located at the center of the quadrupole. The quadrupole length is 0.107 m. The situation is as illustrated in Figure 3.

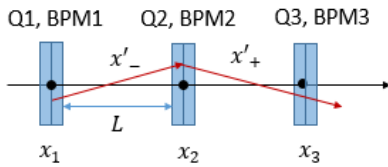


Figure 3: BPMs and quadrupoles in LCLS linac section L3.

Because the quadrupoles are thin and are at the same location as BPMs, the angle coordinates in the drift space can be directly calculated using BPM readings.

$$x'_{-} = \frac{(x_2 - x_1) \frac{3E_1 - E_2}{2E_1}}{L}, \quad x'_{+} = \frac{(x_3 - x_2) \frac{E_3 + E_2}{2E_2}}{L} \quad (1)$$

where $x_{1,2,3}$ are horizontal beam positions at three consecutive BPMs, $E_{1,2,3}$ are beam energies at these locations, x'_{\pm} are horizontal angle coordinates before and after quadrupole Q2 (in Figure 3), and L is the length of the drift space. The strength of the quadrupole Q2 can be derived subsequently from,

$$\Delta x' \equiv x'_{+} - x'_{-} = [KL_q]x_2. \quad (2)$$

The coefficient $[KL_q]$ can be obtained from a linear fitting from trajectory scan data. Figure 4 shows an example using data for one quadrupole in L3.

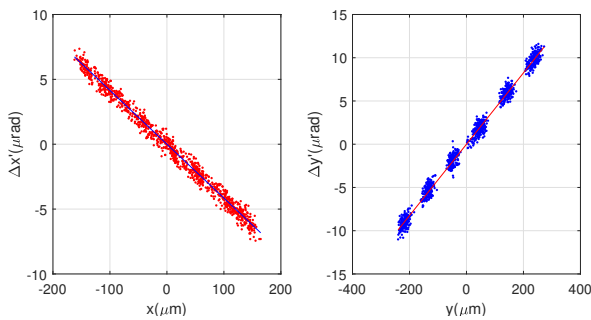


Figure 4: Linear fit of angle coordinate changes vs. position to derive quadrupole strength for one quadrupole in L3.

The effect of the finite length of the quadrupoles can be incorporated using the model strength of the magnets.

Global fitting of tracking data

If the transfer matrix between two BPMs is known, the angle coordinates can be derived from BPM readings. A drift space is the simplest case. The situation in Fig. 3 is another. Knowing the angle and position coordinates of the beam at one BPM, the coordinates at other BPMs can be predicted by tracking through the lattice model. The predicted coordinates can be compared to measurements. The differences can be used to adjust the quadrupole strengths in the model in a fitting scheme.

Because the trajectory shifts at various BPMs for the same trajectory have to be consistent, it is possible to deduce the BPM calibration and roll errors through fitting. At each BPM, the predicted BPM readings (\tilde{x}, \tilde{y}) are related to tracking coordinates (\bar{x}, \bar{y}) by

$$\begin{pmatrix} \tilde{x} \\ \tilde{y} \end{pmatrix} = \begin{pmatrix} \cos \theta & \sin \theta \\ -\sin \theta & \cos \theta \end{pmatrix} \begin{pmatrix} g_x \bar{x} \\ g_y \bar{y} \end{pmatrix}, \quad (3)$$

where θ is the BPM roll and $g_{x,y}$ are horizontal and vertical gains, respectively.

The fitting of the lattice model is a least-square problem, which is aimed at minimizing the objective function

$$\chi^2 = \sum_{n=1}^N \sum_{i=1}^M \left[\frac{x_i(n) - \tilde{x}_i(\mathbf{p})}{\sigma_{x_i}} \right]^2 + \frac{y_i(n) - \tilde{y}_i(\mathbf{p})}{\sigma_{y_i}} \right]^2, \quad (4)$$

where N is the number of trajectories, M is the number of BPMs, \mathbf{p} is a vector of fitting parameters, and $\sigma_{x,y}$ are BPM noise sigma. The least-square problem can be solved with the Levenberg-Marquadt method.

An important note is that adjacent quadrupoles in the lattice model may have a small separation in betatron phase advance and therefore their contributions to the χ^2 have similar patterns and are difficult to resolve. The symptom will show up as small singular values in the Jacobian matrix of the residual vector with respect to the fitting parameters, which in turn lead to large fitted quadrupole errors (ΔK). This can be solved by using constrained fitting which limits the size of ΔK by adding penalty terms to χ^2 [5].

A special issue for one-pass systems is that quadrupoles toward the end of the line are less constrained by the data since a quadrupole only affects the readings on downstream BPMs and there are few BPMs downstream these quadrupoles. One solution may be to use a pair of BPMs at the end of the line to derive the phase space coordinates, track backwards, and combine the comparison with the forward tracking results. The weights of the penalty terms in the constrained fitting for these quadrupoles can also be changed to reduce unreliable excursions in the under-constrained directions.

The fitting approach has been previously tested with a section of a storage ring [3], although there turn-by-turn orbit data were used. The same approach applies to a transport line or a linac as long as the trajectory data sufficiently sample the phase space.

APPLICATION TO LCLS

Here we use LCLS L3 linac data to illustrate the methods described in the previous section. L3 is the acceleration section right after the BC2 bunch compressor which accelerates the beam from 4.5 GeV to the full energy. There are 50 BPMs and 50 Quadrupole magnets in this section, among which BPM 1-47 and Quad 1-47 are at the same locations as shown in Fig. 3. The energy increase between two adjacent quadrupole magnets is approximately 0.2 GeV. The local analysis described in section can be applied here. Figure 5 shows the quadrupole gradient obtained by applying this method to the trajectory scan data. We see good agreement between the measurement and the ideal model except at five quadrupoles (Quad 9-14 in the figure). These quadrupoles were used in optics matching tuning and were thus deliberately changed from their model values.

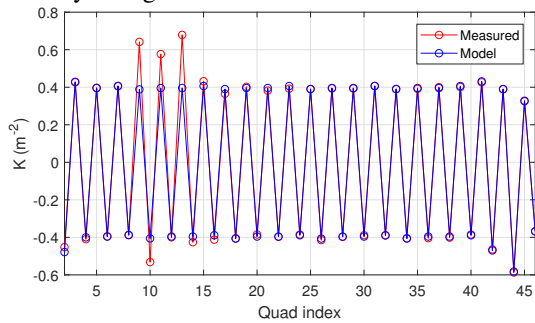


Figure 5: Quadrupole gradients in L3 by local analysis of trajectory data is compared to the ideal model values.

The global fitting method is also applied. There are several locations in LCLS where two BPMs are separated by a drift space. Here the phase space coordinates are derived with BPMs BSY39 (#50) and BSY83 (#53) and are used to track backward using the code AT [6]. Modifications were made to AT to account for the effects of energy change. The fitted quadrupole errors (ΔK) are compared to the local analysis results. The global fitting method also found the same large errors for the five quadrupoles (Fig. 6).

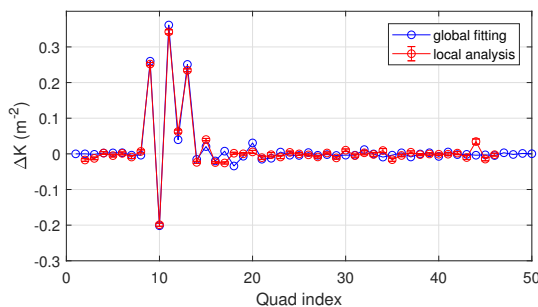


Figure 6: Comparison of ΔK - differences between measured quadrupole gradients and model values - obtained by local analysis and global fitting.

The differences between the measured and tracked trajectories before and after the model is calibrated by fitting are

shown in Fig. 7. There are big differences between measurement and tracking before the large errors for quadrupoles 9-14 are dialed in the model.

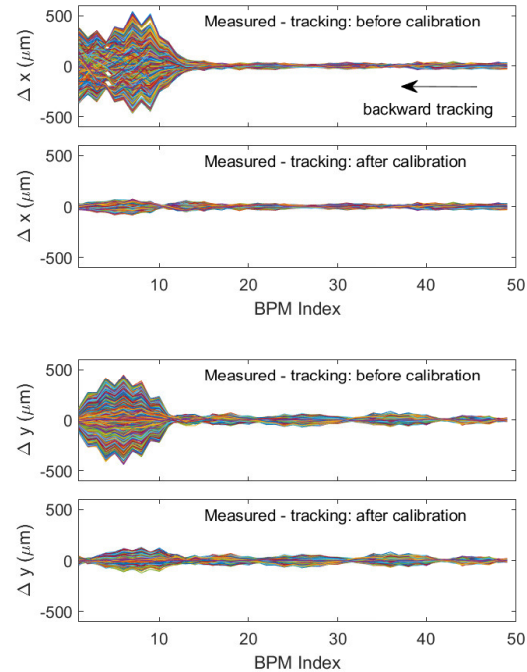


Figure 7: Differences between measurement and tracking before and after model calibration. Tracking is backward.

The global fitting analysis was also performed for three other sections in the LCLS and obtained reasonable results.

SUMMARY

We applied two data analysis methods to process trajectory scan data for the LCLS. One is a local analysis that takes advantage of the fact that in the L3 acceleration section quadrupoles are thin and overlap with BPMs in location which allows us to derive the change of angle coordinates and in turn the quadrupole gradients. The second approach is to derive phase space coordinates using a pair of BPMs separated by a drift space and use them in tracking. The tracked coordinates are compared to measurement in a least-square fitting scheme from which BPM gains and quadrupole strengths can be simultaneously obtained.

The quadrupole error results obtained with the two methods for the LCLS L3 linac agree with each other and are consistent with the operation setting. The quadrupole errors could be used to globally correct the optics errors in the LCLS linac.

REFERENCES

- [1] X. Huang, J. Safranek, W. Cheng, J. Corbett, J. Sebek, Proceedings of PAC09, Vancouver, BC, Canada, 1641-1643, TU6RFP043 (2009).
- [2] J. Safranek, Nucl. Instrum. Meths. A 388 (1-2), 27-36 (1997).

- [3] X. Huang, J. Sebek, D. Martin, Phys. Rev. ST Accel. Beams. 13, 114002, (2010).
[4] P. Emma, W. Spence, Proceedings of PAC 1991, 1549-1551 (1991).
[5] X. Huang, J. Safranek, G. Portmann, ICFA Newsletter 44, 60, (2007).
[6] A. Terebilo, Proceedings of PAC01, Chicago, IL, USA, p. 3203, 2001.